

One-component to two-component transition of the $\nu=2/3$ fractional quantum Hall effect in a wide quantum well induced by an in-plane magnetic field

T. S. Lay

Department of Electrical Engineering, Princeton University, New Jersey 08544

T. Jungwirth and L. Smrčka

Institute of Physics ASCR, Cukrovarnická 10, 162 00 Praha 6, Czech Republic

M. Shayegan

*Department of Electrical Engineering, Princeton University, New Jersey 08544
and Sektion Physik, Ludwig-Maximilians-Universität, D-80539 München, Germany*

(Received 9 May 1997)

The $\nu=2/3$ fractional quantum Hall effect (FQHE) in a wide, single quantum well subject to tilted magnetic fields makes a one-component to two-component transition induced by the in-plane component of the magnetic field. To analyze the experimental data we make a self-consistent, local-density-approximation calculation of the electronic structure of the wide quantum well in tilted magnetic fields. Our results are quantitatively consistent with earlier experimental work on the density driven one-component to two-component FQHE transition in this system. [S0163-1829(97)50536-4]

The development of high-quality, interacting bilayer electron systems has opened a fruitful area of research in the physics of two-dimensional (2D) systems at high magnetic fields.¹⁻⁸ At Landau-level filling factor $\nu=1$, for example, the broken symmetry of the quantum Hall state results in a spontaneous interlayer phase coherence in the absence of tunneling between electron layers.⁶⁻⁸ Another remarkable phenomenon is the fractional quantum Hall effect (FQHE) at even-denominator filling factors³⁻⁵ (e.g., at $\nu=1/2$) which has no counterpart in standard, single-layer 2D systems. The essence of the physics of bilayer systems in the quantum Hall regime is captured by a class of Halperin wave functions^{9,10} $\Phi_{mm'n}$ —a generalization of the Laughlin function for two-component systems. For example, the quantum Hall ferromagnetic state at $\nu=1$ is believed to be described by a fully symmetric orbital function Φ_{111} , while the $\nu=1/2$ FQHE is represented by the Halperin function Φ_{331} .

These quantum Hall states have been observed for bilayer systems either in GaAs double quantum wells separated by an $\text{Al}_x\text{Ga}_{1-x}\text{As}$ barrier or in wide, single quantum wells (WSQW's) of GaAs. For a typical double quantum well structure, the interlayer hopping can be accurately described in the tight-binding approximation (TBA) so that the single-particle problem is fully characterized by two parameters: the tunneling gap Δ_{SAS} and layer separation d . It allows one to make a direct connection to the theory of bilayer quantum Hall liquids, where the different states are identified in the Δ_{SAS} - d phase space. The electronic structure of the system in a WSQW differs from the one in a double quantum well in that the barrier separating the electron layers originates from the Coulomb repulsion of electrons in the well.² This property makes the WSQW particularly intriguing: with increasing electron sheet density, N_s , the height of the effective barrier increases, allowing a transition of the bilayer electron system from a strongly to a weakly coupled one.^{2,3,5} To discuss the FQHE in the WSQW, the low-energy physics can be mapped, for each N_s , onto that of a double quantum well.

The Δ_{SAS} is chosen as equal to the difference between the lowest two energy levels and d is given by the distance between two peaks of the charge distribution in the WSQW. We emphasize that, in the WSQW case, both Δ_{SAS} and d strongly depend on N_s and should be calculated in a self-consistent manner.

The case of certain *even-numerator* FQHE states, such as $\nu=2/3$, is especially interesting in WSQW's and provides the main motivation for experiments presented in this paper. Because of the tunability of the interlayer tunneling, two realizations of the FQHE state are possible in one sample. (i) When Δ_{SAS} is large compared to the intralayer correlation energy $\sim 0.1e^2/4\pi\epsilon\ell_\perp$, where $\ell_\perp = \sqrt{\hbar}/|e|B_\perp$ is the magnetic length, a one-component (1C) state is realized which is the particle-hole conjugate of the standard Laughlin $\nu=1/3$ FQHE state ($2/3=1-1/3$). (ii) For very small $\Delta_{SAS}/(e^2/4\pi\epsilon\ell_\perp)$, a two-component (2C) state is stable consisting of two $\nu=1/3$ FQHE states in two *uncorrelated* layers ($2/3=1/3+1/3$). The 2C state is described by the Halperin wave function Φ_{330} where $n=0$ indicates that there is no interlayer correlation.¹¹

The N_s dependence of the quasiparticle excitation gap $\Delta_{2/3}$ at $\nu=2/3$ in a GaAs WSQW, measured by Suen *et al.*,⁵ clearly shows a 1C to 2C FQHE transition. According to the theory,¹² the above-mentioned 1C and 2C $\nu=2/3$ FQHE states have different topological order and, in an ideal sample, the boundary between them must support a neutral *gapless* liquid state. The experimental data, which were taken only at a few values of N_s , however, do not allow a critical test of whether or not $\Delta_{2/3}$ vanishes at the transition point. Nor do they provide an accurate characterization of the dependence of $\Delta_{2/3}$ on N_s near the transition. The difficulty with obtaining a larger number of experimental points arises from the technically nontrivial task of balancing the electron system for many N_s (by "balanced" we mean a symmetric charge distribution with respect to the center of the WSQW). In this paper we present results of $\nu=2/3$ FQHE measure-

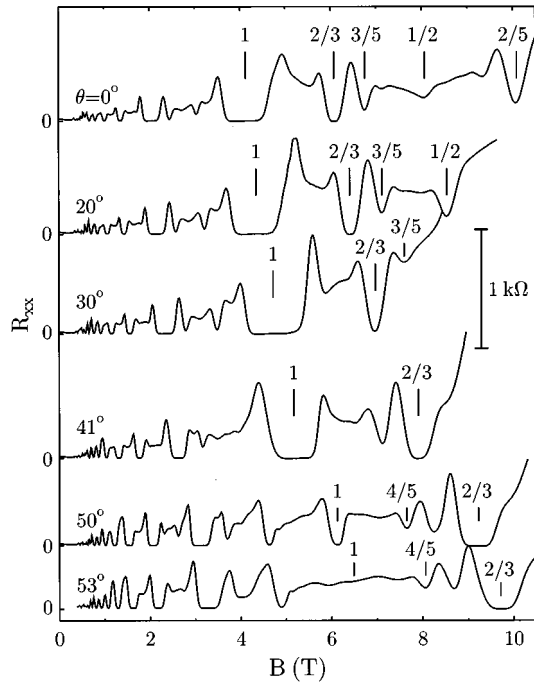


FIG. 1. R_{xx} vs B traces at $T=40$ mK for different tilt angles θ (θ is the angle between B and the normal to the electron layer plane).

ments performed in tilted magnetic fields. Here the 1C to 2C transition is induced in an alternative and experimentally more convenient way by increasing the magnitude of the magnetic field parallel to the 2D electron layer plane while keeping N_s fixed.

The sample we measured was grown by molecular-beam epitaxy and consists of a 75 nm wide GaAs well bounded on each side by undoped (spacer) and Si δ -doped layers of $\text{Al}_{0.35}\text{Ga}_{0.65}\text{As}$.¹³ It has a low-temperature mobility $\sim 1 \times 10^6$ $\text{cm}^2/\text{V s}$. Front-side and back-side gates were used to obtain a balanced charge distribution in the sample. N_s was fixed at 9.8×10^{10} cm^{-2} .

Figure 1 provides an overview of the FQHE observed at $T=40$ mK for different magnetic-field tilt angles θ . Here B is the total magnetic field with the in-plane component $B_{\parallel} = B \sin\theta$. In the measurements, we used an electric current $I=100$ nA. The sample is of exceptionally high quality as it shows very strong FQHE states including the even-denominator $\nu=1/2$ FQHE.⁵ At $\theta=0^\circ$, the $\nu=2/3$ FQHE is well developed. At intermediate $\theta \approx 30^\circ$ it becomes weaker, while for $\theta > 30^\circ$, the $\nu=2/3$ R_{xx} minimum gets wider and deeper again. The quasiparticle excitation gap $\Delta_{2/3}$ was extracted from the slope of the activated temperature dependence of the R_{xx} minimum at $\nu=2/3$, according to $R_{xx} \propto \exp(-\Delta_{2/3}/2T)$. The θ dependence of $\Delta_{2/3}$ is plotted in Fig. 2 revealing a pronounced transition near $\theta=30.5^\circ$. This transition has a striking resemblance to the N_s -driven transition of the $\nu=2/3$ FQHE reported by Suen *et al.*⁵ in the same sample. The origin of the transition is the shrinkage of the tunneling gap Δ_{SAS} which can be induced by either increasing N_s ,⁵ or increasing B_{\parallel} (Fig. 2). In the remainder of the paper, we theoretically analyze the B_{\parallel} -induced transition and show that it is indeed very closely related to the N_s -driven transition.

Qualitatively, the shrinkage of Δ_{SAS} with B_{\parallel} can be seen

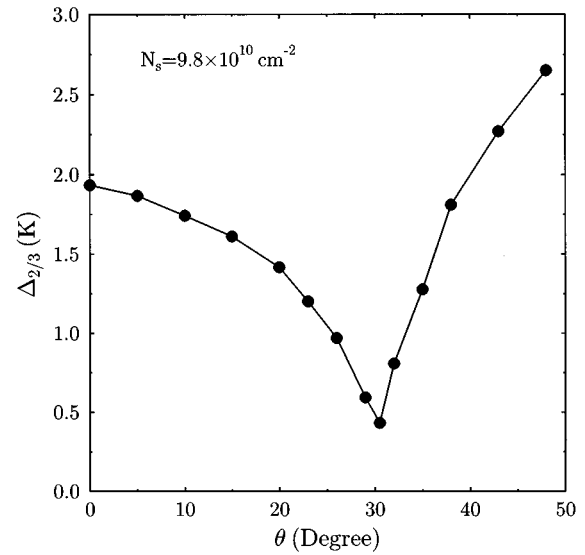


FIG. 2. Measured quasiparticle excitation gap $\Delta_{2/3}$ as a function of the magnetic field tilt angle θ .

from a simple tight-binding-approximation (TBA) model.¹⁴ In the Landau gauge, the vector potential for a tilted magnetic field $\mathbf{B}=(0, B_{\parallel}, B_{\perp})$ reads $\mathbf{A}=(B_{\parallel}z - B_{\perp}y, 0, 0)$. Corresponding wave functions for uncoupled left and right layers are $\psi^{L,R}(x, y) \sim e^{ik_x x} e^{[y - Y^{L,R}(k_x)]^2/2l_{\perp}^2}$. Guiding centers of the Gaussians have a relative shift between the two layers, $|Y^L(k_x) - Y^R(k_x)| = dB_{\parallel}/B_{\perp}$, that is proportional to the strength of the in-plane component of the magnetic field. The decreasing overlap between layer wave functions, i.e., the smaller tunneling rate, yields a reduction of Δ_{SAS} with increasing B_{\parallel} : $\Delta_{SAS}(B_{\parallel}) = \Delta_{SAS}(0) \exp[-(dB_{\parallel}/2l_{\perp}B_{\perp})^2]$. As we will see, however, this expression predicts too rapid of a decrease in Δ_{SAS} with B_{\parallel} . We therefore turn to a self-consistent, local-density-functional approximation (SCLDA) model to calculate the electronic structure of the 75 nm WSQW subject to perpendicular and tilted magnetic fields, and show that the SCLDA model can quantitatively account for the experimental data.

For the perpendicular field configuration, the SCLDA calculation is analogous to that for the zero magnetic-field case.

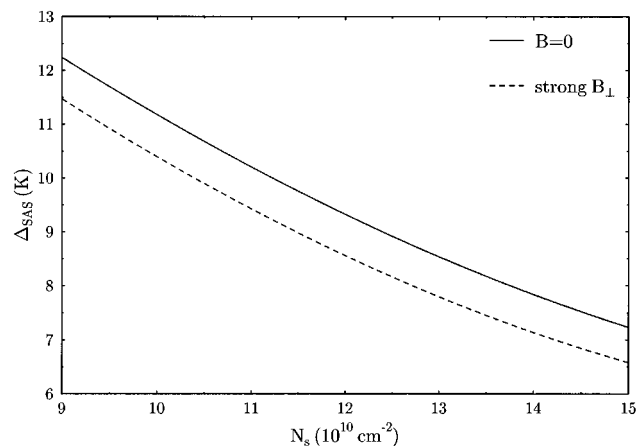


FIG. 3. SCLDA calculation of Δ_{SAS} as a function of the electron sheet density in the wide single well for $B=0$ (solid curve) and strong B_{\perp} (dashed curve).

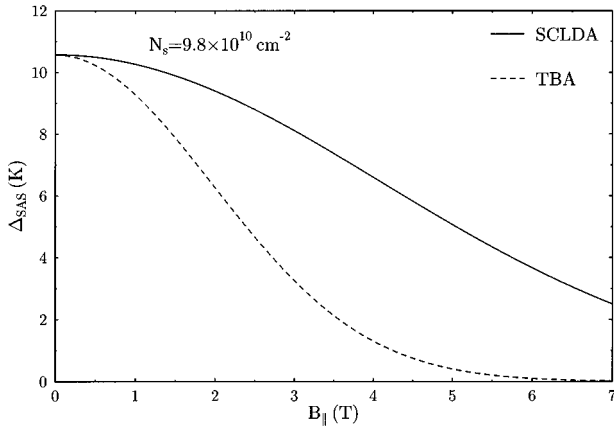


FIG. 4. SCLDA (solid line) and TBA (dashed line) calculation of Δ_{SAS} as a function of the in-plane component of the magnetic field. $B_{\perp} = 6.08$ T.

In-plane (\hat{x} and \hat{y}) and out-of-plane (\hat{z}) components of the electron motion can be decoupled and the eigenstate problem reduces to a numerical solution of a one-dimensional Schrödinger equation for an electron in a potential well. The confining potential of the quantum well, $V_{conf}(z) = V_H(z) + V_{xc}(z)$, is a sum of the Hartree potential and the exchange-correlation term. The electronic structure of the system is obtained from a self-consistent numerical solution of the Schrödinger equation, giving the electron charge distribution, Poisson equation for V_H , and determination of V_{xc} in the local-density-functional approximation. The difference between zero-field and perpendicular magnetic-field results stems from different partitioning of the electronic charge between the lowest two energy states in the quantum well. For the well width and electron sheet densities considered here, both states are populated at zero magnetic field, while at strong magnetic fields ($\nu = 2/3$), the higher-energy state is not occupied.

The computation for the tilted magnetic-field case is more complicated in that there is no gauge for the vector potential which would allow for decoupling of the in-plane and out-of-plane components of the electron motion. Hence, the resulting Schrödinger equation is two-dimensional. To find the eigenstates, we numerically diagonalized the Hamiltonian for an electron subject to combined magnetic and confining electric potentials, using the finite-element method with the linear-spline basis. The potential V_{conf} was obtained in an identical manner to that used for the perpendicular field configuration.¹⁵

We now present the results of our calculations. Figure 3 shows the N_s dependence of the energy gap, Δ_{SAS} , and its renormalization by B_{\perp} . The zero-field curve was obtained using Hedin and Lundquist¹⁶ parametrization of V_{xc} . To calculate Δ_{SAS} at strong B_{\perp} , we assumed that the magnetic field is sufficiently large so that only the lowest, spin-polarized electric subband is occupied, and we applied the Vosko-Wilk-Nusair¹⁷ form of the exchange-correlation energy, which was derived for three-dimensional itinerant ferromagnets. In the considered range of electron sheet densities, Δ_{SAS} is decreased by about 0.8 K due to the strong perpendicular magnetic field. The dependence of Δ_{SAS} on B_{\parallel} , calculated using SCLDA, is shown in Fig. 4. B_{\perp} was

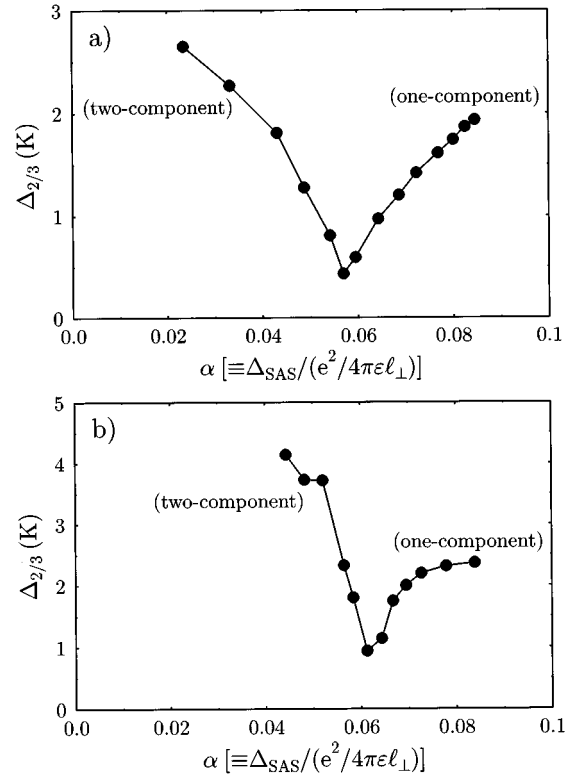


FIG. 5. Plots of measured $\Delta_{2/3}$ vs calculated α , exhibiting the 1C to 2C FQHE transition induced by (a) varying B_{\parallel} , and (b) varying N_s (data of Suen *et al.*, Ref. 5).

fixed at 6.08 T which corresponds to the filling factor $\nu = 2/3$ for $N_s = 9.8 \times 10^{10} \text{ cm}^{-2}$. For comparison, we have also included the results of the TBA model which predicts a much faster collapse of Δ_{SAS} with B_{\parallel} . As the next paragraph will clarify, however, it is the SCLDA that quantitatively accounts for the experimental observations.

The calculated Δ_{SAS} , presented in Figs. 3 and 4, allows us to make a comparison between the results of B_{\parallel} - and N_s -driven experiments. In Fig. 5 we show, for the two experiments, the *measured* quasiparticle excitation gap, $\Delta_{2/3}$, for the $\nu = 2/3$ FQHE state as a function of the parameter $\alpha \equiv \Delta_{SAS} / (e^2 / 4\pi\epsilon\ell_{\perp})$ where Δ_{SAS} is *calculated* via the SCLDA (Figs. 3 and 4).¹⁸ Recall that at sufficiently large values of α the 1C FQHE ensues while at small α the 2C FQHE should be stable. We expect a transition between the two states at $\alpha \sim 0.1$, when Δ_{SAS} becomes comparable to the in-plane correlation energy $\sim 0.1e^2/2\pi\epsilon\ell_{\perp}$. Consistent with this expectation, in Fig. 5 we observe a transition at $\alpha \approx 0.06$. Of particular importance here is that the value of α at the transition is very similar for the B_{\parallel} -induced [Fig. 5(a)] and the N_s -induced [Fig. 5(b)] transitions. If the TBA were used instead to calculate the dependence of Δ_{SAS} on B_{\parallel} , it would shift the $\Delta_{2/3}$ minimum in Fig. 5(a) to $\alpha \approx 0.02$, very far from $\alpha \approx 0.06$ where $\Delta_{2/3}$ exhibits its minimum in the N_s -dependence data [Fig. 5(b)]. We therefore conclude that the FQHE transitions in Figs. 5(a) and 5(b) are similar and that the SCLDA results do quantitatively relate the two together.

It is worth mentioning that the small ($\approx 7\%$) difference between the minima in Figs. 5(a) and 5(b) may be explained

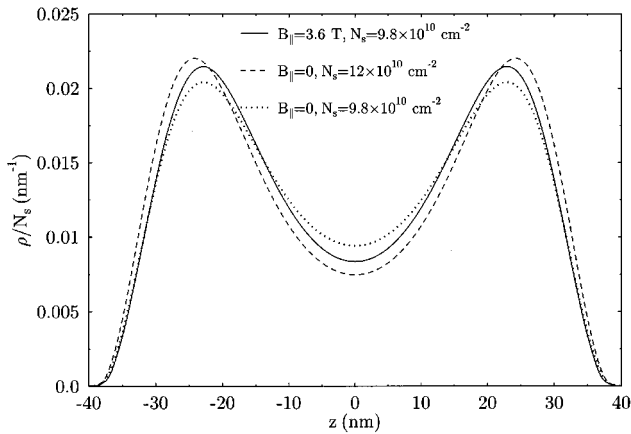


FIG. 6. Charge distribution at the transition points for the tilted magnetic-field experiment (solid curve) and for the N_s -driven experiment of Ref. 5 (dashed curve). The charge distribution for $N_s = 9.8 \times 10^{10} \text{ cm}^{-2}$ at $B_{||} = 0$ is also shown (dotted curve) for comparison (see text).

qualitatively by comparing d/ℓ_{\perp} at the transition points. In the tilted magnetic field experiment, the layer separation d hardly changes with increasing $B_{||}$ (see Fig. 6) and the magnetic length, ℓ_{\perp} , is of course fixed. For the N_s -driven measurement, on the other hand, d increases slightly with increasing N_s (Fig. 6) while ℓ_{\perp} decreases (since the filling factor is fixed at $\nu = 2/3$). Hence, d/ℓ_{\perp} at the transition point is larger (by $\approx 15\%$) than for the $B_{||}$ -driven transition. Theoretical work¹² predicts that for larger d/ℓ_{\perp} the transition between 1C and 2C $\nu = 2/3$ FQHE states occurs at larger α .

This is consistent with what we see when comparing Figs. 5(a) and 5(b).

Finally, we remark on the nonzero value of the measured $\Delta_{2/3}$ at the transition. In the beginning of the paper we mentioned that, for an ideal sample, the theory¹² predicts a gapless liquid state at the boundary between the 1C and 2C $\nu = 2/3$ FQHE states because of the different topological order of the two phases. It is clear in Figs. 5(a) and 5(b) that $\Delta_{2/3}$ does not vanish at the transition point, which is inconsistent with what is theoretically expected for an ideal bilayer system. One possibility is that the 1C $\nu = 2/3$ FQHE state makes a transition to another FQHE state of the same topological order. According to theory,¹² this state would be a pseudospin analog of the single-layer, spin-singlet state. Such a state very rapidly becomes unstable with the introduction of even a slight amount of tunneling and so should hardly be observed in our WSQW system, which has significant tunneling. We surmise, therefore, that sample inhomogeneities and disorder are responsible for the absence of the gapless liquid state in the experimental 1C to 2C transitions that we observe.

The authors are grateful to F. D. M. Haldane, A. H. MacDonald, and K. Yang for stimulating discussions. This work was supported by the National Science Foundation MR-SEC Grant No. DMR-9400362 and Grant No. DMR-9623511, by the National Science Foundation Grant No. INT-9602140, and by the Ministry of Education of the Czech Republic Grant No. ME-104. M. Shayegan acknowledges support from the Alexander von Humboldt Foundation. The experiments were partly performed at the MHMFL, which is supported by NSF Cooperative Agreement No. DMR-9527035, and by the state of Florida.

- ¹G. S. Boebinger *et al.*, Phys. Rev. Lett. **64**, 1793 (1990); A. H. MacDonald, P. M. Platzman, and G. S. Boebinger, *ibid.* **65**, 775 (1990).
- ²Y. W. Suen *et al.*, Phys. Rev. B **44**, 5947 (1991).
- ³Y. W. Suen *et al.*, Phys. Rev. Lett. **68**, 1379 (1992); Y. W. Suen *et al.*, *ibid.* **69**, 3551 (1992).
- ⁴J. P. Eisenstein *et al.*, Phys. Rev. Lett. **68**, 1383 (1992).
- ⁵Y. W. Suen *et al.*, Phys. Rev. Lett. **72**, 3405 (1994).
- ⁶S. Q. Murphy *et al.*, Phys. Rev. Lett. **72**, 728 (1994).
- ⁷K. Yang *et al.*, Phys. Rev. Lett. **72**, 732 (1994).
- ⁸T. S. Lay *et al.*, Phys. Rev. B **50**, 17 725 (1994).
- ⁹S. M. Girvin and A. H. MacDonald, in *Novel Quantum Liquids in Semiconductor Structures*, edited by S. DasSarma and A. Pinczuk (Wiley, New York, 1996).
- ¹⁰B. I. Halperin, Helv. Phys. Acta **58**, 75 (1983).
- ¹¹The physics here has relevance to the reported phase transition for some of the even-numerator FQHE states, such as those at $\nu = 8/5$, $4/3$, and $2/3$ in the standard, single-layer 2D electron systems at the GaAs/Al_xGa_{1-x}As heterojunction: J. P. Eisenstein *et al.*, Phys. Rev. Lett. **62**, 1540 (1989); J. P. Eisenstein *et al.*, Phys. Rev. B **41**, 7910 (1990); R. G. Clark *et al.*, Phys. Rev. Lett. **62**, 1536 (1989); R. G. Clark *et al.*, Surf. Sci. **229**, 25 (1990); J. E. Furneaux, D. A. Syphers, and A. G. Swanson, Phys. Rev. Lett. **63**, 1098 (1989); L. W. Engel *et al.*, Phys. Rev.

- B **45**, 3418 (1992). In the single-layer case, when the density is sufficiently small, these FQHE states occur at low magnetic fields where the Zeeman energy is small compared to the in-plane correlation energy. The states therefore are spin unpolarized and have a 2C origin, the components being real spins. With increasing density, or increasing tilt angle θ between the applied magnetic field and the normal to the 2D plane, these states make a transition to a 1C, spin-polarized state as the Zeeman energy dominates the in-plane correlation energy.
- ¹²I. A. McDonald and F. D. M. Haldane, Phys. Rev. B **53**, 15 845 (1996).
- ¹³We used the same sample as in Ref. 5. Based on all our data, we believe 75 nm is the correct well width for this sample.
- ¹⁴J. Hu and A. H. MacDonald, Phys. Rev. B **46**, 12 554 (1992).
- ¹⁵A detailed study of WSQW's subject to strong B_{\perp} can be found in M. Abolfath, L. Belkhir, and N. Nafari, Phys. Rev. B **55**, 10 643 (1997).
- ¹⁶L. Hedin and B. I. Lundquist, J. Phys. C **4**, 2064 (1971).
- ¹⁷S. H. Vosko, L. Wilk, and M. Nusair, Can. J. Phys. **58**, 1200 (1980).
- ¹⁸In both Figs. 5(a) and 5(b), Δ_{SAS} is calculated for only the symmetric state occupied and with the "ferromagnetic," Vosko-Wilk-Nusair exchange-correlation potential, i.e., the B_{\perp} renormalization of Δ_{SAS} (Fig. 3) is accounted for in both Figs. 5(a) and 5(b).